

Research article

A geometric approach for automatic guidance of marine loading arms

Omid Kavianipour *

Assistant Professor, Department of Mechanical Engineering, Damavand Branch, Islamic Azad University, Damavand, Iran, 3971878911,

*o.kavianipour@damavandiau.ac.ir

(Manuscript Received --- 28 Nov. 2023; Revised --- 28 Dec. 2023; Accepted --- 31 Dec. 2023)

Abstract

In this research the validation of different turbulence models of a hovering propeller at different pitch angles and revolutions has been investigated. For this purpose, the pressure on the propeller surface at different cross sections has been calculated numerically by six different turbulence models and compared with the experimental data. In the first part, the effects of changing the blade angle have been discussed, in this case, the angles of 0, 2, and 12 degrees have been selected. The results showed that changes in the pitch angle of the propeller have led to an increase in the error rate of numerical calculations. At a high pitch angle and in the same chord section, the highest amount of error is produced in leading edge section of the propeller, among which the best model in terms of production error is the k-e RNG. Also, due to the possibility of the formation of shock waves, the S-A and k-e standard models have very large errors, which shows these models' inability to simulate rotating flow with shock waves.

Keywords: Propeller, Blade pitch angle, Turbulence model, Hover, Shock wave.

Nomenclature

a	riser length
b	length of the inboard arm
c	length of the outboard arm
a_1, b_1	location of the first actuator on the MLA
b_2, c_2	location of the second actuator on the MLA
r	distance between the QCDC and the end of the riser length
r_{ac}	amount of expansion and contraction of the actuator
t	time
v_{max}	maximum horizontal velocity of the QCDC
X	position in x coordinate
Y	position in y coordinate
X_0, Y_0	QCDC location in the stored position
X_f, Y_f	Location of the flange of the ship tank
α	angle between the inboard arm and the extension of the riser length
β	angle between the inboard and outboard arms
γ	angle between the inboard arm and r
θ	angle between the riser and r

1- Introduction

These days, one of the common techniques for transfer of cargoes between jetty and

ship is Marine Loading Arms (MLAs). Previously, all-hose structures were used. The disadvantages of these structures are:

continual regulation to keep appropriate hose bend radius, problematic handling, and limited loading rate. MLAs have various configurations because of different goals of coastal production process [1]. This paper focuses on the double-counterweighted, all-metal MLA as shown in Fig 1. It is a three-dimensional articulated structure comprising of a riser which is rigidly fixed at its base, a movable inboard arm attached at the top of the riser, a movable outboard arm connected to the other end of the inboard arm, and two single adjustable counterweights to balance the MLA. Also, MLAs generally have several swivel joints at each end to allow rotation in a vertical plane. All these parts are very heavy, which is why MLAs are usually hydraulically controlled. MLAs have three attitudes, i.e., stored, operating, and maneuvering modes. Once the MLA is statically located at initial position, it is in stored mode. Afterward, the MLA is moved by two hydraulic actuators to connect the Quick Connect-Disconnect Coupler (QCDC) to the flange of the ship tank, as demonstrated in Fig 2. This situation is called operating mode. In maneuvering mode, the QCDC at the tip of the MLA is coupled to the ship flange and then, two actuators are released. This event permits the inboard and outboard arms to follow the normal motion of the moored ship at berth. In operating mode, accurate guidance of the MLA by hydraulic actuators becomes difficult when visibility is impaired by poor lighting situations and stormy weather. Consequently, it is of vital importance to automate conduction of the MLA toward the ship flange in the operating mode with safety and reliability. There are a few researches on the automated controlling system [2] and control strategy [3] for the MLA in the operating mode. Part of the researches is related to the structural

analysis of the MLA. The structural safety of the primary design for the MLA is investigated based on a finite element analysis for the design load conditions in relation to the Oil Companies and International Marine Forum (OCIMF) [4] specifications by Song et. al [5]. Also, Kim et. al [6] performed a structural safety analysis of a MLA by finite element analysis according to the OCIMF for ten load conditions. Choi et. al [7] proposed the new way to design properly the MLA length and the alarm setting considering the mooring motion of the ship. Another area of the researches is the Reliability Centered Maintenance (RCM), which is a maintenance analysis method for the MLA. Siswanto et. al [8] showed that there are three types of maintenance tasks for MLA, i.e., categories A, B, and C which have 14, 21, and zero maintenance tasks, respectively. The American Bureau of Shipping classification [9-10] is utilized for the RCM technique. Eriksen et. al [11] proposed an RCM technique for evaluating reliability challenges and upkeep needs of unmanned cargo ships. Also, a comprehensive explanation of breakdown and downtime terms is given in [12-14]. Failure mode, effect, and criticality analysis (FMECA) is a way applied to evaluate the equipment risk level so that the maintenance strategy can be arranged [15]. Many researchers have developed the FMECA with various methods, for example grey theory [16-17], analytical network process [18], and fuzzy logic [19-20].

The main contribution of this work is to propose a simple and practical method for automatic control of the MLA in the operating mode by hydraulic actuators. To achieve this goal, the two-dimensional system is considered first, and then the

relations necessary for QCDC movement in the direct path from the stored position to the ship flange are extracted. This straight path is the shortest and fastest possible path for the QCDC movement. The only device required to determine this straight line is a position sensor to obtain the coordinates of the tank flange relative to the origin. Then, by applying the extracted equations, the appropriate voltage value is attained for the movement of the hydraulic actuators (by means of the proportional valves), which in turn causes the QCDC to move on a straight line. In this process, the specifications advised by the OCIMF and industry requirements are taken into account.

Structurally, this research features three parts:

The first part pays attention to the length calculation of the inboard and outboard arms according to the MLA datasheet in the industry. Envelope area is illustrated in this section considering MLA alarms. The equations for QCDC movement in the straight line from the stored position to the ship flange are extracted in part two. In the third part, the appropriate voltage value for commanding the hydraulic proportional valves in order to move the hydraulic actuators and then the QCDC linearly is determined.

2- Length of the arms

Based on the technical catalogs of companies active in the oil and gas field, the value of some parameters is requested from customers to determine the dimensions of MLA. These parameters and their definitions are given in Table 1 (values are considered as examples for them in the table). Then, according to the customer's request, the amounts of riser length, inboard arm length, and outboard arm length are calculated.

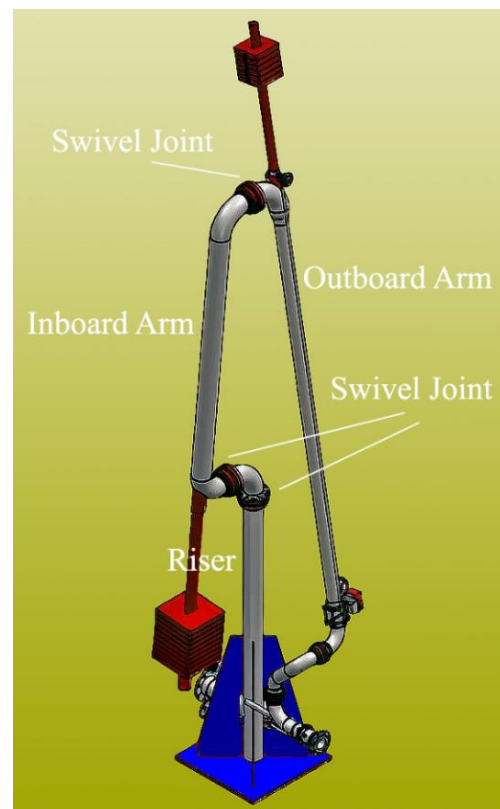


Fig. 1 Double-counterweighted, all-metal marine loading arm

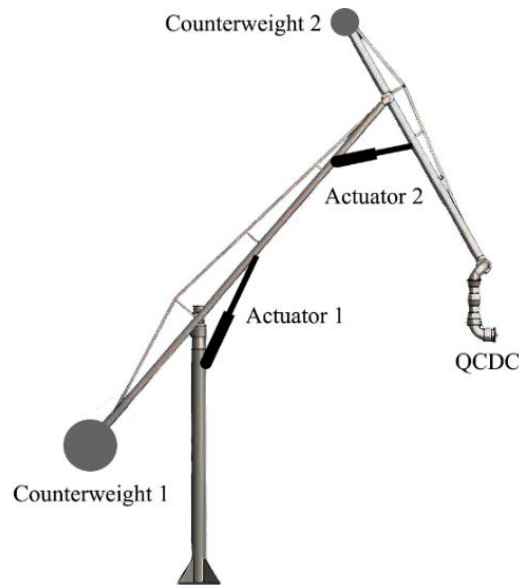


Fig. 2 Two actuators to move the double-counterweighted marine loading arm

Table 1: Typical distance parameter for MLA

Parameter	Value (m)	Definition
<i>A</i>	2.5	Distance: center line of riser to jetty face
<i>B</i>	1.7	Distance: jetty face to berthing line
<i>C</i>	1	Shortest distance: berthing line to ship flange
<i>D</i>	4.6	Widest distance: berthing line to ship flange
<i>E</i>	4.7	Drift range
<i>F</i>	3.8	Distance: jetty level to high tide level (HTL)
<i>G</i>	2.4	Distance: high tide level to low tide level (LTL)
<i>H</i>	1.5	Distance: LTL to center line of ship flange of smallest ship loaded
<i>I</i>	15	Distance: LTL to center line of ship flange of largest ship unloaded
<i>K</i>	3.5	Distance: center line to center line of risers (in case of more than one arm)
<i>L</i>	0.5	Distance: jetty level to connecting flange (land side)
<i>M</i>	1.9	Smallest distance: center line center line of ship flange (in case of more than one arm)
<i>N</i>	5	Widest distance: center line center line of ship flange (in case of more than one arm)

In this section, assuming that the riser length (a) is a certain value and also the angle between the inboard and outboard arms (β_{al}) is specified at the first alarm position of the maneuvering mode by the customer, a procedure for determining the length of the inboard and outboard arms (b and c) is proposed (see Fig. 3).

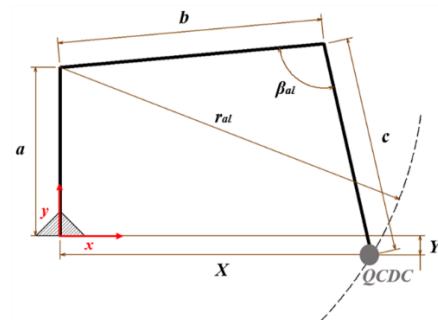


Fig 3. First alarm

According to Fig. 3, when the QCDC is placed on a point with X and Y coordinates, the radius of the circle to the center of the end of the riser length at the first alarm position (r_{al}) can be written as:

$$r_{al} = \sqrt{(a + |Y|)^2 + |X|^2} \quad (1)$$

where $|X|$ and $|Y|$ are equal to $(A + B + C + D - C + E)$ and $(F + G - H)$, respectively.

On the other hand, applying the cosine theorem to the triangle, r_{al} is equal to:

$$r_{al} = \sqrt{b^2 + c^2 - 2bc \cos(\beta_{al})} \quad (2)$$

Therefore, assuming $a = 7$ (m) and $\beta_{al} = 123$ (deg), the “*fmincon*” method in MATLAB software can be used to calculate the values of b and c in accordance with Eq. (3).

$$\begin{cases} \text{function} = \min(b + c) \\ \text{constraint} : b^2 + c^2 - 2bc \cos(\beta_{al}) - r_{al}^2 = 0 \end{cases} \quad (3)$$

Considering a suitable range for the values of b and c , the value of these parameters is equal to 12 (m) and 8.2 (m), respectively.

Finally, knowing the dimensions of the MLA (the values of a , b , and c), the envelope area can be drawn as shown in Fig. 4. In zone 1, after the QCDC is attached to the flange of the ship tank in maneuvering mode, the MLA follows the ship movement due to sea waves (In this regard, mathematical models have been suggested for ship maneuvering [21]). The QCDC enters zone 2 (first alarm) when the value of β_{al} exceeds 123 (deg) as a result of the ship moving away from the jetty. The second alarm occurs in zone 3, when the angle between the inboard and outboard arms is equal to 143 (deg) (this value is specified by the customer). After this angle is increased to a certain extent (for example up to 150 (deg)), the connection between the QCDC and the flange of the ship tank is automatically disconnected.

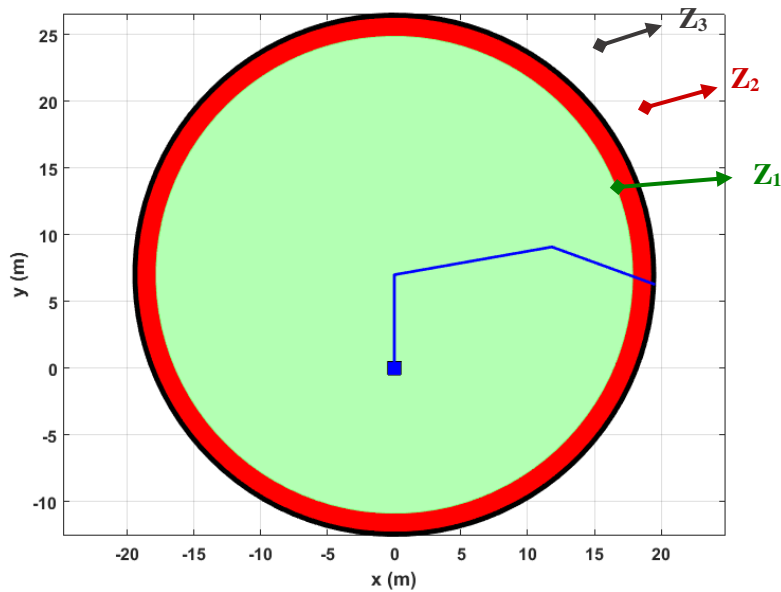


Fig. 4 Envelope area (Z_1 : Zone 1, Z_2 : Zone 2, and Z_3 : Zone 3)

3- Constrained motion of the arms

The main aim of this paper is to offer a simple and practical method for automatic control of the MLA in the operating mode by hydraulic actuators (It should be noted that connection and disconnection of the QCDC with the ship flange is often carried out manually by the operator on the ship or berth). For this purpose, assume that the QCDC is placed on the point with coordinates (X_0, Y_0) in the stored position (see Fig. 5). In Fig. 5, (X_f, Y_f) are the coordinates of the flange of the ship tank at the jetty. The shortest route from point (X_0, Y_0) to point (X_f, Y_f) is the straight path between these two points in the operating

mode. Therefore, if the QCDC moves on this path, it will reach the flange of the ship tank in the fastest time. Considering that the position (X_0, Y_0) is fixed, it is enough to determine the position (X_f, Y_f) with a sensor. In practice, the movement of the ship due to sea waves causes variations in the position (X_f, Y_f) . Using the proposed method in this paper makes the QCDC quickly reach the flange vicinity. After that, the connection of the QCDC with the ship flange is carried out manually by the operator on the ship or berth.

The straight path equation is obtained as follows:

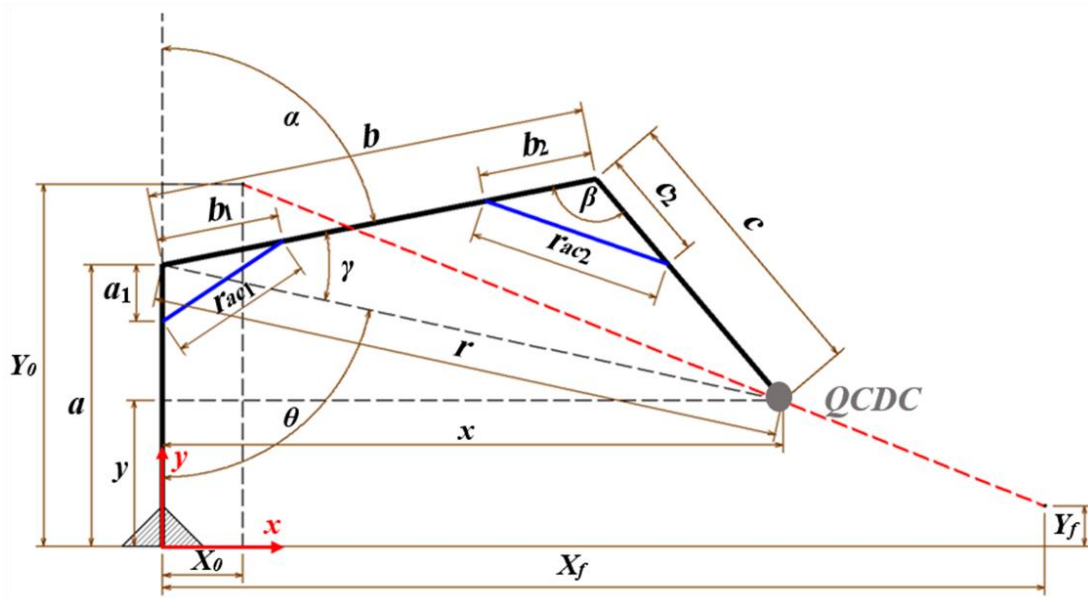


Fig. 5 QCDC motion from the stored position to the flange of the ship tank

$$y = \frac{Y_f - Y_0}{X_f - X_0}(x - X_0) + Y_0 \quad (4)$$

The distance between the QCDC and the end of the riser length (r) is:

$$r = \sqrt{x^2 + (\pm(y - a))^2} \quad (5)$$

where x and y represent the location of the QCDC on the straight path in the two-

dimensional plane relative to the origin. By substituting Eq. (4) in Eq. (5), the value of r depends only on variable x .

On the other hand, applying the cosine theorem to the triangle, r can be written as follows:

$$r = \sqrt{b^2 + c^2 - 2bc \cos(\beta)} \quad (6)$$

where β is the angle between the inboard and outboard arms. It is calculated by Eq. (7).

$$\beta = \arccos\left(\frac{b^2 + c^2 - r^2}{2bc}\right) \quad (7)$$

It is also possible to obtain a relation for c using the cosine theorem for the same triangle.

$$c = \sqrt{r^2 + b^2 - 2rb\cos(\gamma)} \quad (8)$$

γ , which is the angle between the inboard arm, and r is computed by Eq. (9).

$$\gamma = \arccos\left(\frac{b - c\cos(\beta)}{r}\right) \quad (9)$$

Considering the variations of θ (the angle between the riser and r), Eq. (10) is able to express the changes in the values of this parameter in time.

$$\begin{cases} \text{if } (y \geq a) \\ \theta = \arccos\left(\frac{x}{r}\right) + \pi/2 \\ \text{if } (y < a) \\ \theta = \arcsin\left(\frac{x}{r}\right) \end{cases} \quad (10)$$

Finally, the angle between the inboard arm and the extension of the riser length (α) is achieved from the following equation:

$$\alpha = \pi - (\gamma + \theta) \quad (11)$$

Angles α and β play an important role in contraction and expansion values of hydraulic actuators. It should be noted that hitherto the angles α and β are in terms of x . Fig. 6 demonstrates the changes of angle α in terms of angle β for the linear motion of the QCDC on the straight path assuming $X_0 = 3.82$ (m), $Y_0 = 10.40$ (m), $X_f = 14$ (m), and $Y_f = 1$ (m).

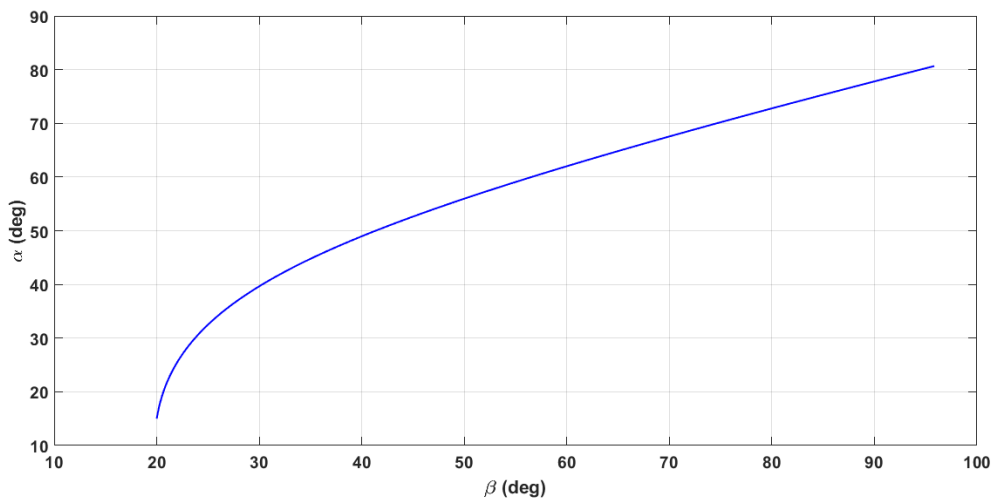


Fig. 6 Changes of angle α versus β

4- Verification using ADAMS

In order to verify the accuracy of the equations derived in the previous section, ADAMS software is utilized here. To reach this goal, a MLA with lengths a , b ,

and c as the riser length, inboard arm length, and outboard arm length are modeled in ADAMS software, respectively. Then, a straight line is drawn between two points (X_0, Y_0) and

(X_f, Y_f) . By using appropriate constraints, the QCDC can be forced to move on this straight line. Finally, the values of angles α (the angle between the inboard arm and the extension of the riser length) and β (the angle between the inboard and outboard arms) are measured at each moment.

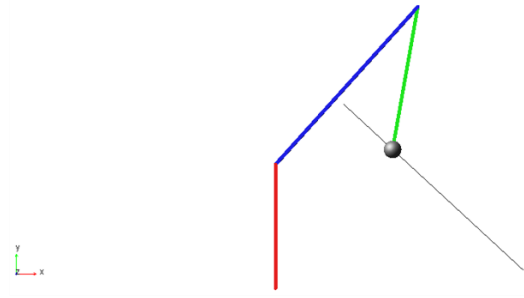


Fig. 7 Simulation in ADAMS

The results attained from the simulation of the QCDC constrained motion in the ADAMS software are illustrated in Fig. 8. As can be seen, the results obtained from the simulation are entirely consistent with the results achieved from solving the equations.

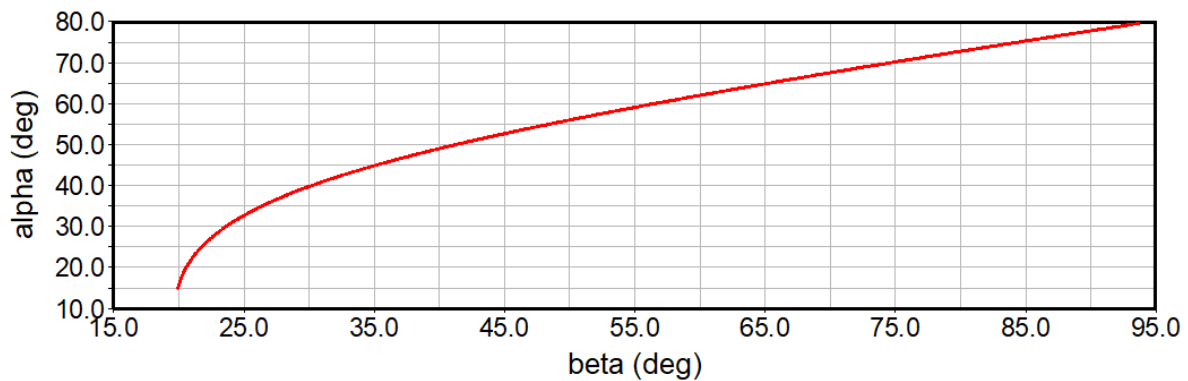


Fig. 8 Results of the simulation

5- Hydraulic actuators motion

As seen in Fig. 5, the amount of contraction and expansion of hydraulic actuators depends on the angles α and β . In other words, the amount of expansion and contraction of the hydraulic actuators must follow a specific pattern to generate the angles α and β shown in Fig. 8 and allow the QCDC to travel in the specified straight path. Therefore, the goal pursued in this section is to calculate the amount of expansion and contraction of the actuators so that the QCDC moves on the straight path.

In Fig. 5, the location of the first and second actuator on the MLA is indicated by the values of a_1 , b_1 , b_2 , and c_2 , respectively. By applying the cosine theorem to the triangle, the amount of expansion and contraction of the first and second actuator (r_{ac1} and r_{ac2}) is computed by Eqs. (12) and (13).

$$r_{ac1} = \sqrt{a_1^2 + b_1^2 - 2a_1b_1 \cos(\pi - \alpha)} \quad (12)$$

$$r_{ac2} = \sqrt{c_2^2 + b_2^2 - 2c_2b_2 \cos(\beta)} \quad (13)$$

Given that the angles α and β are in terms of x , the location variable (x) can be

converted into the time variable (t) by means of the following relationship:

$$\int_{X_0}^x dx = \int_0^t v dt \Rightarrow x = X_0 + v_{\max} t \quad (14)$$

where v_{\max} is the maximum horizontal velocity of the QCDC, which is equal to 0.15 (m/s) based on the OCIMF. Fig. 9 illustrates the variations of r_{ac1} and r_{ac2} for the linear motion of the QCDC on the straight path assuming $a_1 = 1$ (m), $b_1 = 1$ (m), $c_2 = 0.5$ (m), and $b_2 = 1.5$ (m).

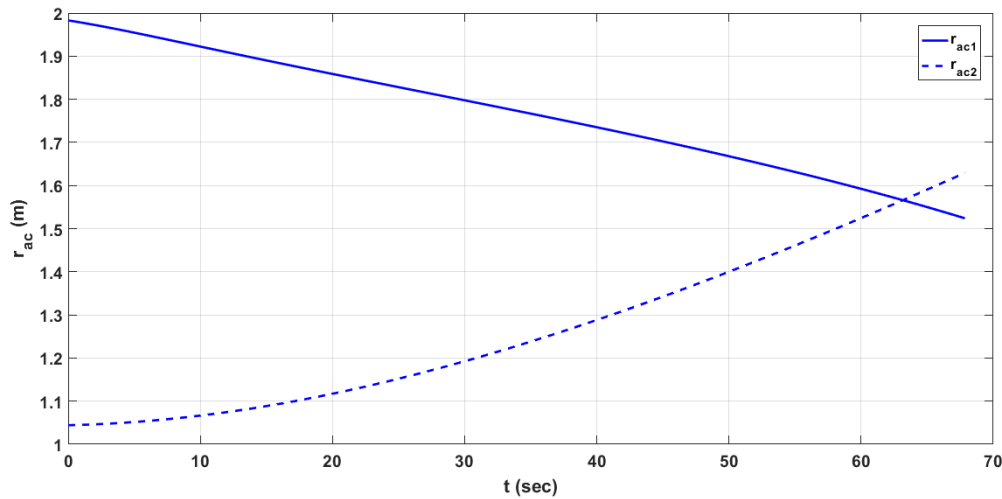


Fig. 9 Contraction and expansion values of hydraulic actuators

According to the amount of expansion and contraction of hydraulic actuators, the appropriate voltage should be calculated to produce these values. For this purpose, it is necessary to convert the gained displacement values with a scale (e.g., a number equal to one) into the required voltage. The amount of this scale depends

on the characteristics of the hydraulic actuator. With this assumption, the estimated voltage values are shown in Fig. 10. Positive voltage means the expansion of the actuator and negative voltage indicates the contraction of the actuator relative to the stored mode (i.e., position (X_0, Y_0)).

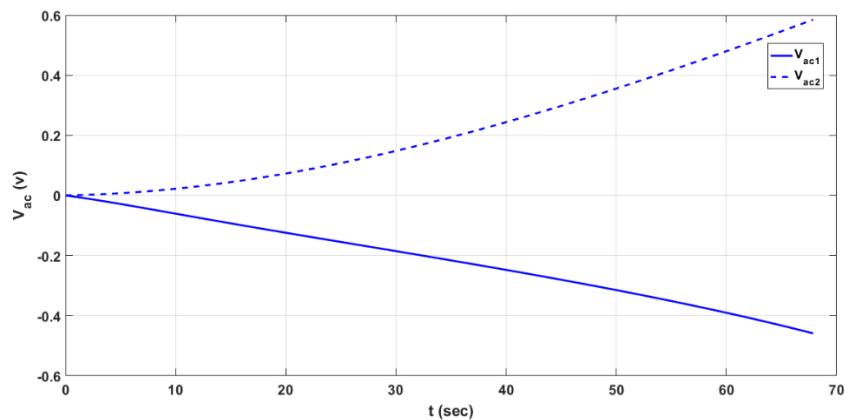


Fig. 10 Required voltage for hydraulic proportional valves

As a matter of fact, the achieved voltage values are the input to an electro-hydraulic system. This system along with its related circuit is demonstrated in Fig. 11. This set consists of 4/3-ways proportional control valve, electrical connection 0 (V), electrical connection 24 (V), function generator (achieved voltage values as an input function), PID controller, pump unit,

double-acting cylinder (as an actuator), displacement encoder, and proportional valve solenoid. In other words, the obtained voltage values are applied as input to an electro-hydraulic system that includes the parts shown in Fig. 11. As a result, the hydraulic actuator expands and contracts to move the QCDC on a predetermined straight path.

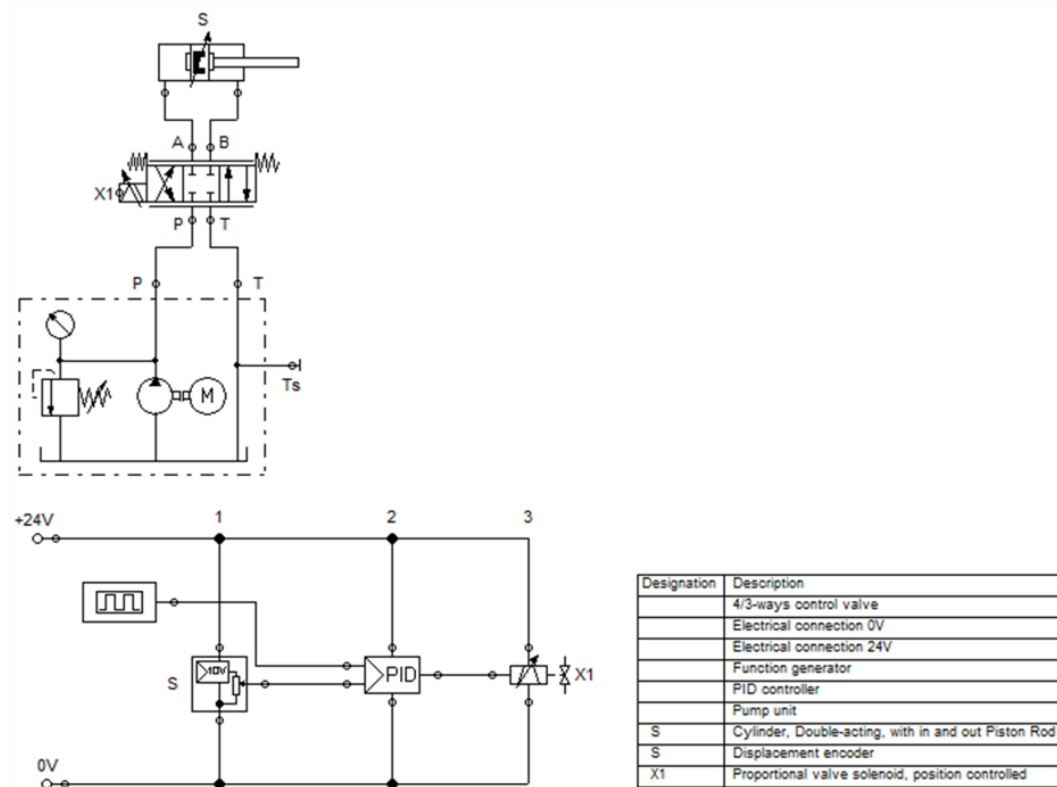


Fig. 11 Electro-hydraulic circuit diagram for the actuator movement

6- Conclusion

This paper focused on an assembly of articulated piping titled Marine Loading Arm (MLA). The main goal of this work was to automate the conduction of a self-supporting MLA balanced via two single adjustable counterweights by means of a simple and practical approach. This proposed approach employed a geometric method to determine the appropriate voltage value to drive the hydraulic actuators, which in turn enabled safe and

rapid movement of the Quick Connect-Disconnect Coupler (QCDC) from the berth toward the coastal tanker flange. To do so, the two-dimensional system was considered first, and then the relations necessary for the QCDC movement in the straight path from the stored position to the ship flange were extracted. This straight path is the shortest and fastest possible path for the QCDC movement. By applying the derived equations, the appropriate voltage value for the movement of hydraulic actuators

stimulated by proportional valves was obtained. In fact, the resulting voltage caused the QCDC to move on a straight line. Finally, the electro-hydraulic circuit diagram for the actuator movement was suggested.

Conflict of interest statement

On behalf of all authors, the corresponding author states that there is no conflict of interest.

References

- [1] Kim, S. W., Park, W. S., Jang, Y. I., Yun, H. D., & Shin, M. Y. (2015). Finite element analysis for structural evaluation of marine loading arm. *Contemporary Engineering Sciences*, 8.
- [2] Sastry, M. K. S., & Seekumar, L. (2012). Automation of real time monitoring and controlling of a marine loading arm. *Journal of Engineering, Design and Technology*, 10(2), 217-227.
- [3] Ugas, N., & Sastry, M. K. S. (2008). A novel control strategy for an ammonia marine loading arm. *The Journal of the Association of Professional Engineers of Trinidad and Tobago*, 37, 60-67.
- [4] Oil Companies and International Marine Forum (OCIMF), Design and Construction Specification for MARINE LOADING ARMS (4th edition), (2019).
- [5] Chang Yong Song, Ha Young Choi and Seung Hwan Shim. (2013). Structural safety evaluation of marine loading arm using finite element analysis. *Journal of Ocean Engineering and Technology*, 27(1), 43-50.
- [6] Kim, S. W., Park, W. S., Jang, Y. I., Yun, H. D., & Shin, M. Y. (2015). Finite element analysis for structural evaluation of marine loading arm. *Contemporary Engineering Sciences*, 8.
- [7] Choi, B. Y., Jo, H. J., Choi, H. S., & Choi, D. E. (2018). A Study on Loading Arm Envelope and Alarm Setting according to Ship Movement. *Journal of Advanced Research in Ocean Engineering*, 4(3), 115-123.
- [8] Siswanto, N., Zaman, M. B., Fahreza, F., Priyanta, D., Pitana, T., Prastowo, H., ... & Fauzi, H. N. (2022). A Case Study Maintenance Task Allocation Analysis on Marine Loading Arm Using Reliability Centered Maintenance. In *IOP Conference Series: Earth and Environmental Science* (Vol. 972, No. 1, p. 012032). IOP Publishing.
- [9] American Bureau of Shipping, Guide for surveys based on machinery reliability and maintenance techniques, (2016).
- [10] American Bureau of Shipping, Guidance notes on reliability-centered maintenance, (2018).
- [11] Eriksen, S., Utne, I. B., & Lützen, M. (2021). An RCM approach for assessing reliability challenges and maintenance needs of unmanned cargo ships. *Reliability Engineering & System Safety*, 210, 107550.
- [12] Pinto, G., Silva, F. J. G., Baptista, A., Fernandes, N. O., Casais, R., & Carvalho, C. (2020). TPM implementation and maintenance strategic plan—a case study. *Procedia Manufacturing*, 51, 1423-1430.
- [13] Bruijn, W. E., Rip, J., Hendriks, A. J., van Gelder, P. H., & Jonkman, S. N. (2019). Probabilistic downtime estimation for sequential marine operations. *Applied Ocean Research*, 86, 257-267.
- [14] Camus, P., Tomás, A., Díaz-Hernández, G., Rodríguez, B., Izaguirre, C., & Losada, I. J. (2019). Probabilistic assessment of port operation downtimes under climate change. *Coastal Engineering*, 147, 12-24.
- [15] Siswanto, N., & Zaman, M. B. (2020). Criticality assessment for marine diesel engine using failure mode and effect criticality analysis (FMECA) approach: Case study on lubricating oil system. *International Review of Mechanical Engineering*, 14(4), 258-263.

- [16] Li, X., Li, H., Sun, B., & Wang, F. (2018). Assessing information security risk for an evolving smart city based on fuzzy and grey FMEA. *Journal of Intelligent & Fuzzy Systems*, 34(4), 2491-2501.
- [17] Liu, H. C., Wang, L. E., You, X. Y., & Wu, S. M. (2019). Failure mode and effect analysis with extended grey relational analysis method in cloud setting. *Total Quality Management & Business Excellence*, 30(7-8), 745-767.
- [18] Alrifayy, M., Sai Hong, T., Supeni, E. E., As' array, A., & Ang, C. K. (2019). Identification and prioritization of risk factors in an electrical generator based on the hybrid FMEA framework. *Energies*, 12(4), 649.
- [19] Liu, H., Deng, X., & Jiang, W. (2017). Risk evaluation in failure mode and effects analysis using fuzzy measure and fuzzy integral. *Symmetry*, 9(8), 162.
- [20] Zaman, M. B., Kobayashi, E., Wakabayashi, N., Khanfir, S., Pitana, T., & Maimun, A. (2014). Fuzzy FMEA model for risk evaluation of ship collisions in the Malacca Strait: based on AIS data. *Journal of Simulation*, 8(1), 91-104.
- [21] Hajizadeh, S., Seif, M. S., & Mehdigholi, H. (2016). Determination of ship maneuvering hydrodynamic coefficients using system identification technique based on free-running model test. *Scientia Iranica*, 23(5), 2154-2165.